DTU Informatics
Department of Informatics and Mathematical Modeling

Measuring growth in mice with craniofacial dysmorphology caused by the Crouzon mutation $Fgfr2^{C342Y}$

Signe Thorup[a,b], Hildur Ólafsdóttir[a], Tron Darvann[b], Nuno Hermann[b,c], Per Larsen[b], Rasmus Paulsen[a,b] Chad A. Perlyn[d], Sven Kreiborg[b,c,e], Rasmus Larsen[a]
[a] DTU Informatics, Technical University of Denmark, Lyngby, Denmark
[b] 3D Craniofacial Image Research Laboratory (School of Dentistry, University of Copenhagen; Copenhagen University Hospital Rigshospitalet; and DTU Informatics, Technical University of Denmark), Copenhagen, Denmark
[c] Pediatric Dentistry and Clinical Genetics, School of Dentistry, Faculty of Health Sciences, University of Copenhagen, Denmark
[d] Division of Plastic Surgery, Washington University School of Medicine, St. Louis, MO, USA
[e] Department of Clinical Genetics, The Juliane Marie Centre, Copenhagen University Hospital Rigshospitalet, Copenhagen, Denmark

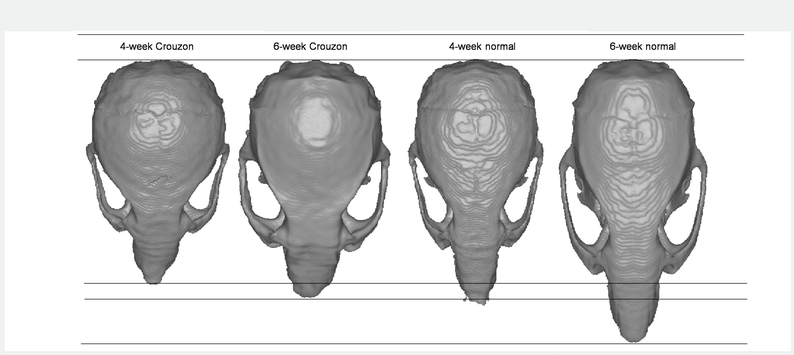

Figure 1: Calculated mean surfaces (atlases) from each mouse group. Notice how much the average normal mouse changes from 4 to 6 weeks of age, compared to the Crouzon mice. The surfaces were extracted from micro-CT scans using the Marching Cube Algorithm [4].

Introduction

Crouzon syndrome is a genetic disease causing premature fusion of the cranial sutures leading to growth disturbances. The syndrome has an incidence of 1:64.500 live births [1].
In 1994 the gene causing Crouzon syndrome was discovered, and a mouse model was introduced in 2004 [2].
Previous studies have validated the mouse model as a suitable model for studying the syndrome [3].
The purpose was to compare growth between Crouzon syndrome (*Fgfr2* $^{C342Y/+}$) and a control group of normal mice.

Material

The data consists of 3D micro CT scans of 30 mouse skulls – 10 four week and 20 six week old mice. Each age group consists of 50% wild-type (normal) mice and 50% Crouzon mice. The material is cross-sectional: the mice were euthanized before they were CT scanned. See Figure 1 for

Method

Using rigid and non-rigid image registration [5,6,7] correspondences were constructed between the mouse images - either for atlas building as in Figure 1 or for generating growth vectors as in Figure 3.

The registration accuracy was examined using landmarks. Rohlfing [Rohlfing2012] stated that, unlike most evaluation methods, a dense set of landmarks is the ideal way of detecting incorrect registrations. A clinical expert familiar with landmarking annotated the set of images with 49 anatomical landmarks according to Figure 2. The landmarks on the 6-week-old normal atlas were propagated to all subjects using the obtained deformation fields. Subsequently, landmark errors were estimated. The errors are defined by the Euclidean distance between an automatically obtained landmark and the corresponding manual landmark. Most errors were found to be less than 0.5 mm.

18 skull parameters were measured using the annotated landmarks, see Figure 4.

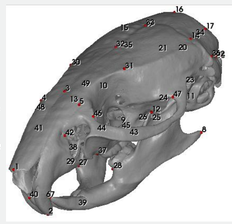

Figure 2: The 49 landmarks used for validating the registration and measuring skull parameters. The landmarks are shown on the 6-week normal atlas.

Results

Looking at the growth rates for SL and NL, the Crouzon mice grew at approximately half the normal rate. SH, SW, and IOD are approximately twice the normal rate. MX growth rate was approximately eight times larger for normal mice; the negative rate for the Crouzon mice is probably a result of bone resorption. MW2 growth rate was almost three times larger for Crouzon mice. MW1, MH, IODp were almost a quarter larger than the normal rate. Crouzon mice were inhibited in growth for MLM, ML1, and Z, while NW growth increased compared to normal growth. Finally, MW3, ML2, ML3 and ICD had equal growth rates according to a t-test.

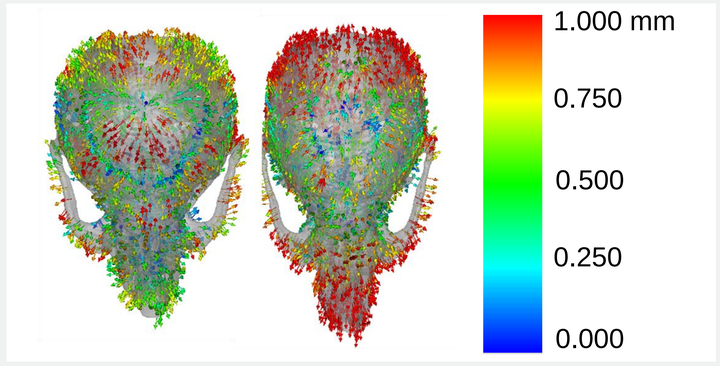

Figure 3: Every 200th deformation vector shown on 4-week-old atlases. Left: The 4-week-old normal atlas with growth vectors. Right: The 4-week-old Crouzon atlas. The colors denote displacement with respect to atlas (in mm), with red denoting most change (>= 1 mm) and purple no change.

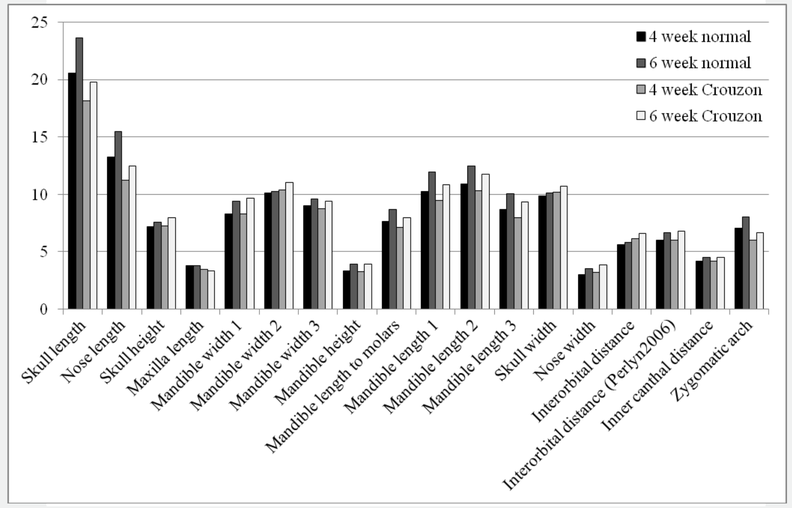

Figure 4 Diagram showing the magnitude of the 18 skull parameters. All parameters are measured in millimeters. Black bins denote 4-week-old normal mice, dark gray bins denote 6-week-old normal mice, light gray bins denote 4-week-old Crouzon mice, and white bins denote 6-week-old Crouzon mice.

Skull parameter	Abbreviations	Landmarks
Skull length	SL	34-40
Nasal length	NL	40-45
Skull height	SH	16-24
Maxilla length (left/right)	MX	37/38-43/44
Mandible width 1-3	MW1-3	8-9, 10-11, 12-13
Mandible height (left/right)	MH	8/9-11/10
Mandible length to 1st molars (left/right)	MLM	11/10-28/27
Mandible length 1-3 (left/right)	ML1-3	8/9-39, 11/10-39, 12/13-39
Skull width	SW	35-36
Nose width	NW	42-41
Interorbital distance	IOD	31-30
Interorbital distance (Perlyn 2006)	IODp	46-48
Inner canthal distance	ICD	5-4
Zygomatic arches (left/right)	Z	46/48-47/49

Conclusion

We have built a model for automatic phenotyping using appropriate registration models. This model confirmed our knowledge of Crouzon development in mice, for the first time.

The Crouzon mice clearly had a different growth pattern, a difference caused by the fused sutures; e.g. skull and nose length were inhibited. Skull height, for instance, was rated equal for 4-week-old mice; while at 6 weeks, the skull height had increased for Crouzon mice. Other measures, such as skull width, revealed compensatory growth meaning that the Crouzon mice grew more than normally excepted. With the automatically placed landmarks, we were able to estimate the growth rate for Crouzon and normal mice. For example, skull length and nose width grew almost half as much for Crouzon mice compared to normal mice. On the other hand, skull width and interorbital distance grew twice as much for Crouzon mice.

Acknowledgement
For all image registrations the Image Registration Toolkit was used under license from Ixico Ltd.

References
[1] Editor D. P. Rice. Craniofacial sutures. Development, disease and treatment. Krager 2008.
[2] V. P. Eswarakumar, M. C. Horowitz, R. Locklin, G. M. Morriss-Kay, P. Lonai. A gain-of-function mutation of *Fgfr2c* demonstrates the role of this receptor variant in osteogenesis. Proceedings of the National Academy of Sciences of the United States of America, 34(101):12555-12560, 2004.
[3] H. Ólafsdóttir. Analysis of craniofacial images using computational atlases and deformation fields. Ph.D. thesis, DTU, 2007.
[4] Lorensen WE, Cline HE (1987). Marching cubes: A high resolution 3D surface construction algorithm. ACM SIGGRAPH Computer Graphics 21(4), 163-9.
[5] C. Studholme, D.L.G.Hill, D.J. Hawkes, An Overlap Invariant Entropy Measure of 3D Medical Image Alignment, Pattern Recognition, Vol. 32(1), Jan 1999, p. 71-86.
[6] D. Rueckert, L. I. Sonoda, C. Hayes, D. L. G. Hill, M. O. Leach, and D. J. Hawkes. Non- rigid registration using free-form deformations: Application to breast MR images. IEEE Transactions on Medical Imaging, 18(8):712-721, 1999.
[7] J. A. Schnabel, D. Rueckert, M. Quist, J. M. Blackall, A. D. Castellano Smith, T. Hartkens, G. P. Penney, W. A. Hall, H. Liu, C. L. Truwit, F. A. Gerritsen, D. L. G. Hill, and D. J. Hawkes. A generic framework for non-rigid registration based on non-uniform multi-level free-form deformations. In MICCAI 2001, p. 573-581.
[8] T. Rohlfing. Image similarity and tissue overlaps as surrogates for image registration accuracy: Widely used but unreliable. IEEE Transactions on Medical Imaging, 31(2):153-163, 2012.